



A Comparative Analysis of LSTM and GRU Models for AQI Forecasting in Tourist Destinations

Luluk Ardianto*, Yani Parti Astuti

Faculty of Computer Science, Informatics Engineering, Universitas Dian Nuswantoro, Semarang, Indonesia

Email: ^{1,*}luluxs42@gmail.com, ²yanipartiastuti@dsn.dinus.ac.id

Correspondence Author Email: luluxs42@gmail.com

Submitted: 06/01/2025; Accepted: 03/05/2025; Published: 01/06/2025

Abstract—The Air Quality Index (AQI) is a critical metric for assessing air quality and its impact on human health, particularly in densely populated and tourist-heavy areas such as Malioboro, Yogyakarta. As one of Indonesia's most popular tourist destinations, the region experiences significant air quality fluctuations influenced by human activities, including transportation and tourism. This study evaluates the performance of two advanced deep learning models, Long Short-Term Memory (LSTM) and Gated Recurrent Unit (GRU), in forecasting AQI and key pollutant parameters, PM10 and PM2.5, using two years of air quality data collected between January 2022 and December 2023. The results demonstrate that the LSTM model consistently outperforms GRU in predicting AQI (MSE: 163.757, RMSE: 12.797, MAE: 7.432, MAPE: 0.133) and PM2.5 (MSE: 32.001, RMSE: 5.657, MAE: 3.005, MAPE: 0.139), indicating its capability to model complex temporal patterns effectively. Conversely, the GRU model achieves better accuracy for PM10 predictions (MSE: 58.592, RMSE: 7.655, MAE: 4.168, MAPE: 0.180), showcasing its computational efficiency with competitive performance. These findings underscore the suitability of LSTM for applications prioritizing accuracy, while GRU provides a viable option for scenarios requiring faster computations. This research highlights the potential of leveraging deep learning models to tackle air quality challenges in urban and tourist areas, paving the way for informed decision-making and sustainable development initiatives

Keywords: AQI; Forecasting; GRU; LSTM; Tourist Destination

1. INTRODUCTION

The Air Quality Index (*AQI*) is a critical environmental health indicator that reflects the level of air cleanliness and its potential impact on human health [1]. The AQI is influenced by the concentration of Particulate Matter (*PM*), including both PM10 and PM2.5, which originate from vehicle emissions, household combustion, and road dust [2]. Other factors, such as Carbon Monoxide (*CO*), Sulfur Dioxide (*SO₂*), Nitrogen Dioxide (*NO₂*), and Ozone (*O₃*), also contribute to air quality [3]. A high AQI value indicates poor air quality, which can have adverse effects on human health [4]. In the context of tourism, the AQI plays a significant role, particularly for destinations that receive both domestic and international travelers. Tourist attractions with good air quality are generally preferred, as they offer a more comfortable experience, enhance the competitiveness of the destination, and contribute to higher visitor satisfaction [5].

In the city of Yogyakarta, the Malioboro tourist area is one of the most popular destinations, attracting both domestic and international tourists [6]. According to the 2024 report by the Special Region of Yogyakarta (DIY) Province, the number of visitors recorded at Malioboro from January to November 2024 reached 4.6 million, including both domestic and international tourists. This high volume of visitors has contributed to poor air quality in the area, primarily due to vehicle emissions, tourism activities, and population density. The convergence of these environmental factors, compounded by rising temperatures characteristic of Yogyakarta, poses a significant threat to public health, both among tourists and local residents [7]. Based on these factors, air quality prediction is very important in identifying and reducing the impact of pollution that can affect health in the Malioboro area. It is therefore important to understand these patterns and trends if effective mitigation measures are to be implemented to ensure healthy air is maintained for the benefit of the community and its visitors [8].

Machine Learning (*ML*) and Deep Learning (*DL*) have recently emerged as popular methods for AQI prediction, due to their proven effectiveness and efficiency [9]. Previous studies have applied various ML techniques such as Random Forest, Support Vector Regression (*SVR*), and CatBoost Regression, develop reasonably accurate predictions[10]. Other traditional models like SARIMA and Support Vector Machine (*SVM*) have also been employed with promising results in AQI forecasting [11]. However, recent research has shown that neural network-based models often outperform traditional ML methods in capturing nonlinear patterns and long-term dependencies in time series data [12] Consequently, deep learning models such as Convolutional Neural Networks (*CNN*), Deep Neural Networks (*DNN*), and Denoising Autoencoders (*DAE*) have been explored in the context of air pollution forecasting [13], Sedangkan Several Neural Network-based models commonly used include Long Short-Term Memory (*LSTM*) and Gated Recurrent Unit (*GRU*) [14]. Among these, Long Short-Term Memory (*LSTM*) and Gated Recurrent Unit (*GRU*) are particularly favored for their strength in sequence modeling.

A comparison of the two algorithms reveals that they utilize different approaches to make predictions [15]. The LSTM model utilizes memory cells and three gates (input, output, and forget) to effectively manage long-term dependencies in time series data, thereby enhancing prediction accuracy [16]. This approach enables LSTM to demonstrate higher accuracy when handling complex and flexible data [17]. Meanwhile, the GRU model utilizes a



reduced set of two gates, specifically the Reset and Output gates, to make predictions [18]. This makes the GRU model more computationally efficient, as it uses fewer parameters [19].

Despite the success of deep learning models in AQI prediction, many existing studies fall short in performing comprehensive optimization, particularly in aspects such as data splitting strategies and hyperparameter tuning. These limitations can affect the generalizability and robustness of model performance in diverse environmental settings.

This study aims to address these gaps by systematically comparing the performance of two recurrent neural network architectures, LSTM and GRU, for AQI forecasting in Malioboro, a highly dynamic tourist area in Yogyakarta, Indonesia. Through various experimental setups, the research seeks to identify the most effective model for generating reliable and timely air quality information, which can be used to support environmental monitoring and pollution mitigation strategies in urban tourism destinations.

2. RESEARCH METHODOLOGY

2.1 Dataset

This study uses a two-year air quality observation dataset from the Malioboro area in Indonesia. The dataset was obtained through the public Application Programming Interface (*API*) of Weatherbit.io. The dataset covers the period from January 2022 to December 2023. Data were collected monthly and consolidated into a single JSON dataset containing a total of 17,258 entries. A detailed explanation of the features in the dataset is provided in Table 1, while a sample of the dataset is presented in Figure 1.

Table 1. Description of Dataset Feature

No	Feature	Descriptions
1	Aqi	General air quality levels based on pollutants (PM2.5, PM10, O ₃ , NO ₂ , CO, and SO ₂)
2	CO	Carbon monoxide concentration (ppm)
3	Datetime	Air quality data measurement time
4	NO2	Nitrogen Dioxide concentration level (μg/m ³)
5	O3	Ozone concentration level (μg/m ³)
6	PM10	Air particles with a diameter of ≤ 10 micrometers (μg/m ³)
7	PM2.5	Air particles with a diameter of ≤ 2.5 micrometers (μg/m ³)
8	SO2	Sulfur dioxide concentration (μg/m ³)

```

GRU_Malioboro_Single.ipynb   { maliboro_2022-2023.json }

{ maliboro_2022-2023.json > [ ] data > {} 0
  1 {
  2   "city_name": "Yogyakarta",
  3   "country_code": "ID",
  4   "data": [
  5     {
  6       "aqi": 173,
  7       "co": 175.9,
  8       "datetime": "2022-01-31T17",
  9       "no2": 32,
 10       "o3": 8.7,
 11       "pm10": 102,
 12       "pm25": 72.67,
 13       "so2": 65,
 14       "timestamp_local": "2022-02-01T00:00:00",
 15       "timestamp_utc": "2022-01-31T17:00:00",
 16       "ts": 1643648400
 17     }
  ],
}

```

Figure 1. Example of Dataset

2.2 Purpose Method

The dataset obtained through the API is subjected to a preprocessing stage to ensure that only relevant data is used in the analysis. Initially in JavaScript Object Notation (JSON) format, the data is converted into a DataFrame to facilitate data analysis. Columns that are deemed irrelevant are subsequently removed to reduce data complexity. This step aims to simplify the dataset by eliminating unnecessary columns. Exploratory Data Analysis (EDA) is performed to validate the data types in each column, ensuring their consistency with the values before processing. The next step involves data cleaning, which includes checking and handling missing values and outliers, to ensure the dataset maintains its quality [20]. The Datetime column is set as the index, and the data is sorted in ascending order based on time before the processing stage. Feature selection is performed using a heatmap correlation to filter relevant features based on their high correlation levels [21]. Data normalization is also performed to ensure that all features have a clean dataset with consistent value scales [22]. The cleaned dataset is processed using sequencing techniques to form historical data

sequences for predicting AQI values. The LSTM and GRU models are trained with various experimental schemes, such as differences in data splitting and variations in learning rates, to find the most optimal results in predicting air quality.

The following evaluation metrics were utilized in this study: Mean Squared Error (*MSE*), Root Mean Squared Error (*RMSE*), Mean Absolute Error (*MAE*), and Mean Absolute Percentage Error (*MAPE*). The purpose of employing these metrics was to assess the model's performance in predicting AQI. *MSE* quantifies the average squared difference between predicted and actual values, with smaller values indicating smaller prediction errors [23]. *RMSE*, as the square root of *MSE*, represents the model's error in the same units as the AQI data, where smaller values indicate more accurate predictions [24]. Furthermore, *MAE* calculates the mean absolute deviation between the predicted and actual values, with smaller values indicating a greater degree of similarity between the model's predictions and the actual values [25]. The mean absolute percentage error (*MAPE*) evaluation metric is employed to evaluate the model's accuracy by assessing the error between the actual and predicted values in percentage form [26]. An overview of the entire research flow, from data preprocessing, modeling, to evaluation, can be seen in Figure 2.

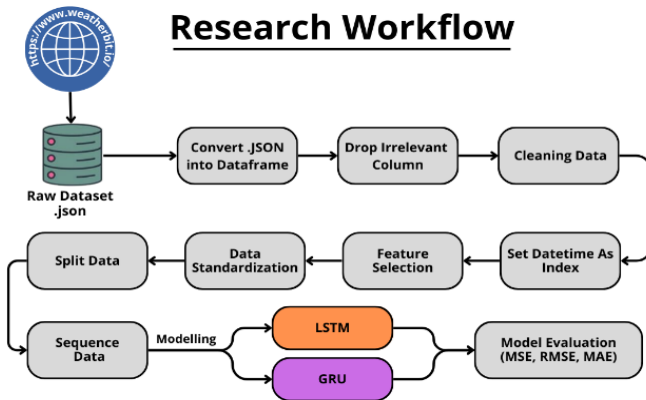


Figure 2. Research Workflow

2.3 Long Short Term Memory (LSTM)

Long Short-Term Memory (LSTM) is a type of artificial neural network architecture designed to model sequential data [27]. In several studies, LSTM has shown good performance in detecting AQI [28]. LSTM has three types of gates: the input gate, output gate, and forget gate, which play a crucial role in regulating the flow of information, these gates determine which information is stored, forgotten, and passed on to maintain context during data processing [29].

$$i(t) = \sigma(w(i) * [x(i), h(i-1)] + b(i)) \quad (1)$$

$$C(i) = \tanh(w(c) * [x(i), h(i-1)] + b(i)) \quad (2)$$

$$f(t) = \sigma(w(f) * [x(t), h(t-1) + b(f)]) \quad (3)$$

$$C(t) = i(t) * C(t) + f(t) * C(t - 1) \quad (4)$$

$$o(t) = \sigma(W(o) * [x(t), h(t-1)] + b(o)) \quad (5)$$

$$h(t) = \phi(t) * \tanh(C(t)) \quad (6)$$

Equations 1 through 6 describe the mathematical mechanisms in the LSTM model based on the functions of each gate [30]. Equation (1) represents the *input gate* $i(t)$ which uses the sigmoid function to determine how much new information $C(i)$ will be added to the memory cell. This information is calculated using the \tanh activation function in Equation (2), where the current input $x(t)$ and the previous hidden state $h(t-1)$ are combined with the relevant weights and biases. Next, the *forget gate* $f(t)$. In Equation (3) controls how much of the old information $C(t-1)$ will be retained or forgotten from the memory cell.

The cell state memory $C(t)$ is updated with contributions from the *input gate* and *forget gate*, as expressed in Equation (4). The information stored in the cell state is then used to compute the new hidden state. Finally, in the *output gate* $O(t)$ as shown in Equation (5), the sigmoid function is used to determine which portion of the cell state will be sent as output. The final output or hidden state $h(t)$ is computed by combining the value of $O(t)$ and the cell state, which is activated using the tanh function, as formulated in Equation (6). The cell state, which has been activated using the tanh function as formulated in Equation (6), is then combined with the output gate. Therefore, the interplay of the input gate, forget gate, and output gate in LSTM allows the model to store important information over the long term, disregard irrelevant information, and generate accurate outputs for prediction or classification on sequential data [31]. An illustration of the operational mechanism of the LSTM model from equations 1 to 6 can be seen in Figure 3.

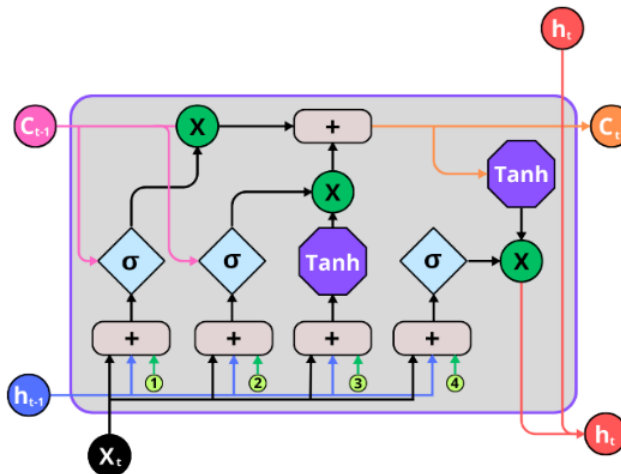


Figure 3. LSTM Work Diagram

2.4 Gated Recurrent Unit (GRU)

Gated Recurrent Unit (GRU) is a type of deep learning architecture that utilizes a gating mechanism. Unlike LSTM, GRU uses only two types of gates: the update gate and the reset gate [32]. The two gates are complementary in their management of Flexible Memory, with the Update gate retaining salient information and the Reset gate removing less pertinent data. This ensures that the GRU model maintains its focus on the relevant context. [33]. In certain AQI detection scenarios, the GRU model has demonstrated enhanced performance in comparison to other conventional models, such as SVM, RNN, and LSTM, in achieving evaluation effectiveness [34].

$$U_t = \sigma(W_r * [h_{t-1}, x_t]) \quad (7)$$

$$Z_t = \sigma(W_z * [h_{t-1} + x_t]) \quad (8)$$

$$H_t^* = \tanh (W_h^* * [r_t \otimes h_{t-1}, x_t]) \quad (9)$$

$$H_t = (1 - z_t) \otimes h_{t-1} + z_t \otimes H_t^* \quad (10)$$

Equations 7 through 10 represent a mathematical formulation of the operational mechanism of the Gated Recurrent Unit (GRU) [35]. In Equation (7), the update gate (U_t) determines the information to be updated based on the current input (x_t) and the previous hidden state (h_{t-1}). Meanwhile, in Equation (8), the reset gate (Z_t) controls how much information from the hidden state will be passed on to the candidate hidden state calculation (H_t^*). The next process is that (H_t^*) is calculated using Equation (9), considering the influence of the reset gate. The final hidden state (H_t) is then obtained through a linear combination of (H_t^*) and the previous hidden state (h_{t-1}) with weights determined by the update gate (U_t) as shown in Equation (10). This structure ensures that relevant information is retained while unnecessary information is discarded, thus improving computational efficiency without compromising performance. [36]. An illustration of the operational mechanism of the GRU model from equations 7 to 10 can be seen in Figure 4.

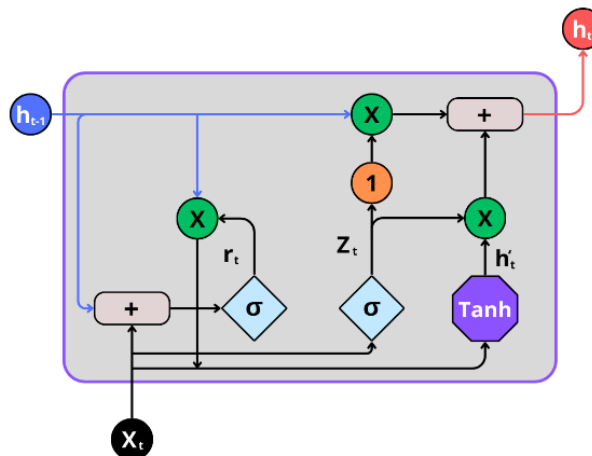


Figure 4. GRU Work Diagram



3. RESULT AND DISCUSSION

3.1 Result

Several columns in the dataset, such as "city_name," "country_code," "lat," "lon," "state_code," "timezone," "timestamp_local," "timestamp_utc," and "ts," are irrelevant and thus dropped. The remaining dataset consists of 8 key columns: "aqi," "co," "datetime," "no2," "o3," "PM10," "PM2.5," and "so2." Among the columns analyzed, there are 75 missing values and several outliers across all columns, except for "datetime." Missing values are handled by removing the data, while outliers are retained as they remain within acceptable limits and could provide useful information for the forecasting process.



Figure 5. Heatmap Correlation

As illustrated in Figure 5, a heatmap correlation analysis was conducted to identify three primary columns with elevated correlation levels for the AQI forecasting process: "aqi," "pm10," and "pm25." Subsequent to the feature selection stage, the data is partitioned into multiple data splitting scenarios for training and testing, with ratios of 60:40, 70:30, and 80:20. The MinMaxScaler from the Sklearn library is employed to standardize the data, ensuring that all feature values fall within the range of 0 to 1. This procedure is performed to ensure the stability and consistency of the data during the model training process. Sequencing is applied using 24 hours of data to predict the subsequent 3 hours values. This approach is employed for both LSTM and GRU models, where both models are tested with different learning rate schemes: 0.01, 0.001, and 0.0001. In this experiment, the batch size is standardized to 64, with the Adam optimizer.

The best results from the LSTM and GRU models were found in the data splitting scenario of 70% for training and 30% for testing. The experimental results can be seen in Table 2 for a learning rate of 0.0001, in Table 3 for a learning rate of 0.001, and in Table 4 for a learning rate of 0.01.

Table 2. Experiment Result with 0.0001 learning rate

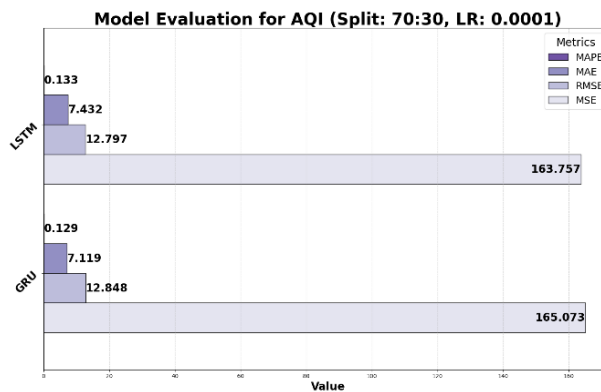
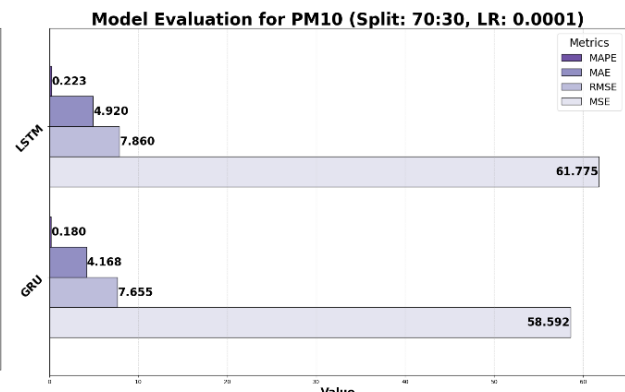
Model	Data Train : Data Test	Learning Rate	Metric	MSE	RMSE	MAE	MAPE
LSTM	70 : 30	0.0001	AQI	163.756	12.796	7.4319	0.1329
	70 : 30	0.0001	PM10	61.7751	7.8597	4.9201	0.2226
	70 : 30	0.0001	PM2.5	32.0011	5.6569	3.0049	0.1931
	70 : 30	0.0001	AQI	165.078	12.848	7.1189	0.1293
GRU	70 : 30	0.0001	PM10	58.5917	7.6545	4.1678	0.1804
	70 : 30	0.0001	PM2.5	33.4736	5.7856	2.7787	0.1706

Table 3. Experiment Result with 0.001 learning rate

Model	Data Train : Data Test	Learning Rate	Metric	MSE	RMSE	MAE	MAPE
LSTM	70 : 30	0.001	AQI	211.898	14.556	7.6472	0.1336
	70 : 30	0.001	PM10	90.7201	9.5247	5.7582	0.2730
	70 : 30	0.001	PM2.5	48.2731	6.9479	3.7365	0.2509
	70 : 30	0.001	AQI	237.996	15.427	9.4653	0.1908
GRU	70 : 30	0.001	PM10	80.7812	8.9878	4.5086	0.2148
	70 : 30	0.001	PM2.5	49.3581	7.0255	3.9275	0.2869

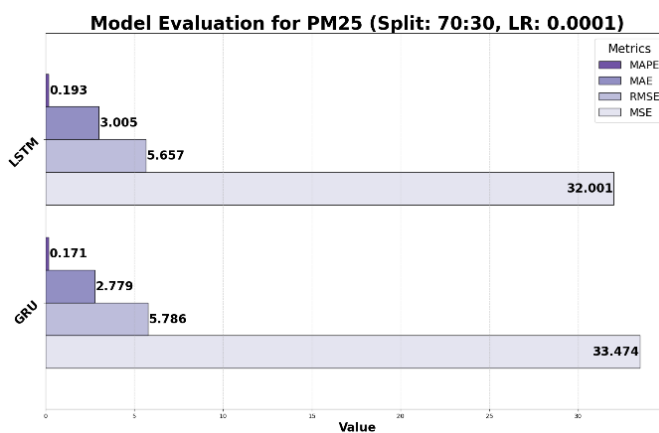
**Table 4.** Experiment Result with 0.01 learning rate

Model	Data Train : Data Test	Learning Rate	Metric	MSE	RMSE	MAE	MAPE
LSTM	70 : 30	0.01	AQI	294.390	17.157	9.9832	0.1661
	70 : 30	0.01	PM10	96.5012	9.8235	6.6138	0.2785
	70 : 30	0.01	PM2.5	55.1641	7.4273	4.0778	0.2321
GRU	70 : 30	0.01	AQI	468.206	21.638	18.796	0.3965
	70 : 30	0.01	PM10	123.992	11.1352	8.5843	0.4469
	70 : 30	0.01	PM2.5	80.8652	8.9925	7.3900	0.5952

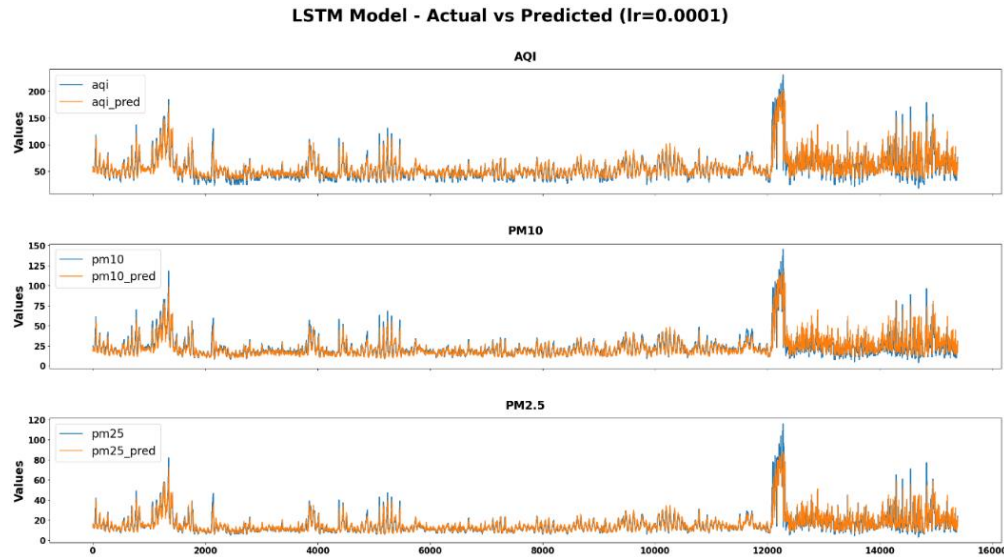
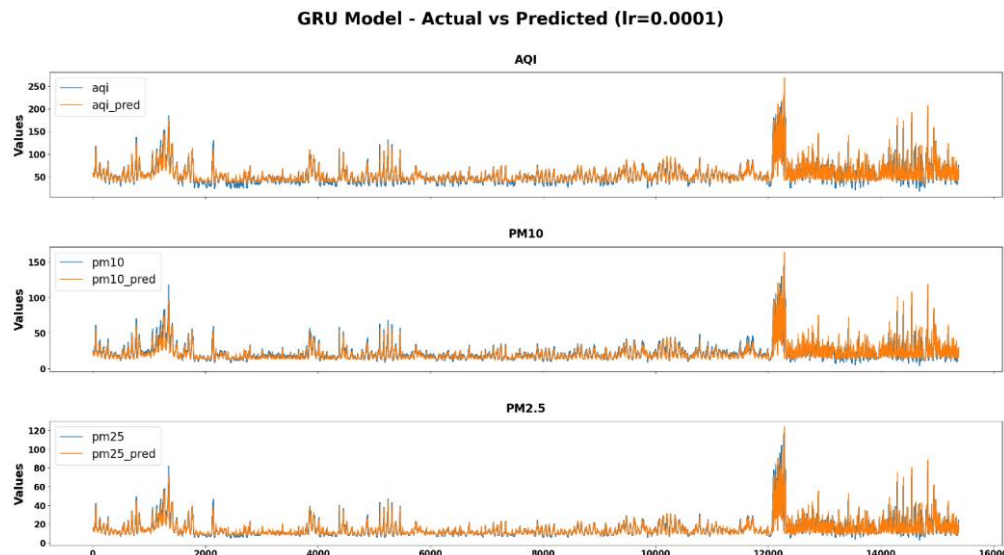
**Figure 6.** AQI Best Model**Figure 7.** PM10 Best Model Result

Based on the illustration in Figure 6, the LSTM model demonstrates the best performance in AQI prediction evaluation under the 70:30 data splitting scenario with a learning rate of 0.0001. The model achieves a Mean Squared Error (MSE) of 163.757, a Root Mean Squared Error (RMSE) of 12.797, a Mean Absolute Error (MAE) of 7.432, and a Mean Absolute Percentage Error (MAPE) of 0.133. These results indicate that the LSTM model exhibits relatively low prediction errors for AQI compared to the other evaluated models.

Furthermore, as illustrated in Figure 7, the model evaluation for PM10 prediction shows that the GRU model outperforms the LSTM model overall. This is evident from the GRU's lower error values, achieving an MSE of 58.592, an RMSE of 7.655, an MAE of 4.168, and a MAPE of 0.180, compared to the LSTM results. These findings suggest that while the performance gap between LSTM and GRU in AQI prediction is relatively small, the GRU model provides superior performance in PM10 prediction tasks, making it a more optimal choice for this specific case.

**Figure 8.** PM2.5 Best Model Result

As illustrated in Figure 8, the evaluation results for PM2.5 prediction show an opposite trend compared to those for PM10. In this case, the LSTM model achieves better performance than the GRU model, with an MSE of 32.001, an RMSE of 5.657, an MAE of 3.005, and a MAPE of 0.193. These results indicate that the LSTM model is more capable of accurately predicting PM2.5 values within the given experimental setup. Meanwhile, the GRU model also performs competitively but with slightly higher error metrics, where the MSE, RMSE, and MAE are recorded at 33.474, 5.786, and 2.779, respectively. A deeper evaluation of both models is presented in Figures 9 and 10, where Figure 9 focuses on the best results from the LSTM model, and Figure 10 highlights the best performance achieved by the GRU model. Overall, these findings help provide a clearer picture of how each model behaves when predicting PM2.5 under similar conditions.

**Figure 9.** Best Model LSTM Forecasting**Figure 10.** Best Model GRU Forecasting

3.2 Discussion

A previous study indicated that the LSTM model demonstrated the most optimal performance in forecasting weather conditions across various locations in Pati, Indonesia. The LSTM model utilized in that study exhibited a Mean Squared Error (MSE) of 94.248, a Root Mean Squared Error (RMSE) of 9.708, and a Mean Absolute Error (MAE) of 6.036 [28]. Several testing scenarios in previous research showed that the LSTM model tends to perform better than the GRU model. This is attributed to the more complex architecture of LSTM, which enables the model to capture time series data relationships more effectively [37]. In this study, the performance of both LSTM and GRU models in predicting the Air Quality Index (AQI) in the Malioboro area was evaluated. The LSTM model attained an MSE of 163.757, an RMSE of 12.797, and a Mean Absolute Error (MAE) of 7.097, with a Mean Absolute Percentage Error (MAPE) of 12.9%. In comparison, the GRU model exhibited slightly higher errors, with an MSE of 165.073, an RMSE of 12.848, and an MAE of 7.119, along with a MAPE of 12.9%. While the differences between the two models are relatively minor, the results indicate that the LSTM model has a slight edge in predictive accuracy. This aligns with previous findings that attribute LSTM's superior performance to its more complex architecture, which effectively captures long-term dependencies in time series data. This advantage is particularly relevant for air quality forecasting in tropical climates like Malioboro, where seasonal weather patterns, high humidity, and fluctuating air quality due to tourism and transportation activities play a significant role. Additionally, this study evaluated key pollutant parameters, PM10 and PM2.5, which are critical indicators of air quality. The identification of the most accurate model for AQI prediction is a critical step in developing effective data-driven solutions for mitigating air pollution in tourist areas. This research contributes to this effort by providing a framework for identifying accurate models.



4. CONCLUSION

The experimental results demonstrate the efficacy of both Long Short-Term Memory (LSTM) and Gated Recurrent Unit (GRU) models in predicting the Air Quality Index (AQI), as well as PM10 and PM2.5 concentrations. The LSTM model, with its more complex architecture, exhibited superior performance in predicting AQI, achieving an MSE of 163.757 and an RMSE of 12.797. Furthermore, LSTM demonstrated higher performance in predicting PM2.5 compared to GRU, as evidenced by metrics such as MSE of 32.001, RMSE of 5.657, MAE of 3.005, and MAPE of 0.193. In contrast, the GRU model excelled in predicting PM10, achieving an MSE of 58.592, RMSE of 7.655, MAE of 4.168, and MAPE of 0.180. These results highlight the strengths of both models: LSTM is recommended for applications requiring high predictive accuracy, especially for AQI and PM2.5, while GRU offers a viable alternative in scenarios that prioritize computational efficiency without significant loss in accuracy. This study demonstrates the efficacy of deep learning models in addressing air quality challenges, particularly in tourist areas such as Malioboro. Future research should explore hybrid approaches or fine-tuning strategies to further optimize performance for specific air quality parameters under diverse environmental conditions.

REFERENCES

- [1] M. Chen, “Analyzing the Daily Air Quality Index in the U.S. in Time Series,” *Highlights Sci. Eng. Technol.*, vol. 88, pp. 1297–1302, 2024, doi: 10.54097/m6y2hj11.
- [2] S. Rana, “Determination of Air Quality Life Index (Aqli) in Medinipur City of West Bengal(India) During 2019 To 2020 : A contextual Study,” *Curr. World Environ.*, vol. 17, no. 1, pp. 137–145, 2022, doi: 10.12944/cwe.17.1.12.
- [3] D. Seng, Q. Zhang, X. Zhang, G. Chen, and X. Chen, “Spatiotemporal prediction of air quality based on LSTM neural network,” *Alexandria Eng. J.*, vol. 60, no. 2, pp. 2021–2032, 2021, doi: 10.1016/j.aej.2020.12.009.
- [4] Y. Zhang, M. Yang, F. Yang, and N. Dong, “A Multi-step Prediction Method of Urban Air Quality Index Based on Meteorological Factors Analysis,” *E3S Web Conf.*, vol. 350, 2022, doi: 10.1051/e3sconf/202235001010.
- [5] Y. Su and C. C. Lee, “The impact of air quality on international tourism arrivals: a global panel data analysis,” *Environ. Sci. Pollut. Res.*, vol. 29, no. 41, pp. 62432–62446, 2022, doi: 10.1007/s11356-022-20030-6.
- [6] M. L. Afandi, J. Wibowo, C. Candraningrat, and A. Supriyanto, “Analisis Hubungan Atribut Destinasi Wisata Terhadap Kepuasan Wisatawan Pada Kawasan Malioboro,” *Sadar Wisata J. Pariwisata*, vol. 6, no. 2, pp. 89–97, 2023, doi: 10.32528/sw.v6i2.1200.
- [7] S. Patimah, A. Shinta, and A. G. Rizqia, “Psikologi Lingkungan : Pentingkah Untuk Dipelajari ?,” *Jurnal Psikologi*, vol. 20, no. 2, pp. 108–112, 2024.
- [8] Michel, “Perbandingan Metode Prophet Dan Long Short Term Memory (Lstm) Dalam Peramalan Kualitas Udara (Studi Kasus Kualitas Udara Kota Bandar Lampung),” *Repositori Universitas Lampung*, vol. 4, no. 1, pp. 1–23, 2024.
- [9] A. Pant, S. Sharma, and K. Pant, “Evaluation of Machine Learning Algorithms for Air Quality Index (AQI) Prediction,” *J. Reliab. Stat. Stud.*, vol. 16, no. 2, pp. 229–242, 2023, doi: 10.13052/jrss0974-8024.1621.
- [10] N. S. Gupta, Y. Mohta, K. Heda, R. Armaan, B. Valarmathi, and G. Arulkumaran, “Prediction of Air Quality Index Using Machine Learning Techniques: A Comparative Analysis,” *J. Environ. Public Health*, vol. 2023, pp. 1–26, 2023, doi: 10.1155/2023/4916267.
- [11] N. N. Maltare and S. Vahora, “Air Quality Index prediction using machine learning for Ahmedabad city,” *Digit. Chem. Eng.*, vol. 7, no. November 2022, p. 100093, 2023, doi: 10.1016/j.dche.2023.100093.
- [12] M. AL-Ghamdi, A. A. M. AL-Ghamdi, and M. Ragab, “A Hybrid DNN Multilayered LSTM Model for Energy Consumption Prediction,” *Appl. Sci.*, vol. 13, no. 20, 2023, doi: 10.3390/app132011408.
- [13] G. Isam Drewil and R. Jabbar Al-Bahadili, “Multicultural Education Forecast Air Pollution in Smart City Using Deep Learning Techniques: A Review,” *Multicult. Educ.*, vol. 7, no. 5, pp. 38–47, 2021, doi: 10.5281/zenodo.4737746.
- [14] J. Wang, X. Li, L. Jin, J. Li, Q. Sun, and H. Wang, “An air quality index prediction model based on CNN-ILSTM,” *Sci. Rep.*, vol. 12, no. 1, pp. 1–16, 2022, doi: 10.1038/s41598-022-12355-6.
- [15] S. Nosouhian, F. Nosouhian, and A. K. Khoshouei, “A review of recurrent neural network architecture for sequence learning: Comparison between LSTM and GRU,” *Preprints.org*, no. July, pp. 1–7, 2021, doi: 10.20944/preprints202107.0252.v1.
- [16] S. Raut, “Stock Market Price Prediction and Forecasting Using Stacked LSTM,” *Interantional J. Sci. Res. Eng. Manag.*, vol. 08, no. 03, pp. 1–5, 2024, doi: 10.55041/ijssrem29832.
- [17] Z. Wang, “Stock price prediction using LSTM neural networks: Techniques and applications,” *Appl. Comput. Eng.*, vol. 86, no. 1, pp. 294–300, 2024, doi: 10.54254/2755-2721/86/20241605.
- [18] W. A. Degife and B. S. Lin, “Deep-Learning-Powered GRU Model for Flight Ticket Fare Forecasting,” *Appl. Sci.*, vol. 13, no. 10, 2023, doi: 10.3390/app13106032.
- [19] N. Hussein and A. M. Abdulazeez, “Bitcoin Price Prediction Using Hybrid LSTM-GRU Models,” *Indones. J. Comput. Sci.*, vol. 13, no. 1, pp. 94–101, 2024, doi: 10.33022/ijcs.v13i1.3725.
- [20] K. Paul, “Data Expedition: Travel Through Data Preprocessing, EDA And PCA,” *Educ. Adm. Theory Pract.*, vol. 30, no. 6, pp. 2576–2590, 2024, doi: 10.53555/kuey.v30i6.5828.
- [21] S. BUYRUKOĞLU and A. AKBAŞ, “Machine Learning based Early Prediction of Type 2 Diabetes: A New Hybrid Feature Selection Approach using Correlation Matrix with Heatmap and SFS,” *Balk. J. Electr. Comput. Eng.*, vol. 10, no. 2, pp. 110–117, 2022, doi: 10.17694/bajece.973129.
- [22] F. A. Kusuma, “Pemodelan Klasifikasi Anemia Aplastik Menggunakan Teknik Oversampling Dan K-Nearest Neighbors,” *J. Inform. dan Tek. Elektro Terap.*, vol. 12, no. 3, 2024, doi: 10.23960/jitet.v12i3.4326.
- [23] Das Pankaj, “Performance Metrics in Predictive Modeling,” 2024, [Online]. Available: <https://orcid.org/0000-0003-1672-2502>
- [24] T. O. Hodson, “Root-mean-square error (RMSE) or mean absolute error (MAE): when to use them or not,” *Geosci. Model Dev.*, vol. 15, no. 14, pp. 5481–5487, 2022, doi: 10.5194/gmd-15-5481-2022.



- [25] S. M. Robeson and C. J. Willmott, "Decomposition of the mean absolute error (MAE) into systematic and unsystematic components," *PLoS One*, vol. 18, no. 2 February, pp. 1–8, 2023, doi: 10.1371/journal.pone.0279774.
- [26] C. Tofallis, "A better measure of relative prediction accuracy for model selection and model estimation," *J. Oper. Res. Soc.*, vol. 66, no. 8, pp. 1352–1362, 2015, doi: 10.1057/jors.2014.103.
- [27] O. E. C. Mary, "a Framework for Decoding Physiological and Neural Signal Using Long Short-Term Memory (Lstm)," *Int. J. Adv. Res. Comput. Sci.*, vol. 14, no. 03, pp. 114–118, 2023, doi: 10.26483/ijarcs.v14i3.6986.
- [28] I. W. Ramadhan *et al.*, "Forecasting Air Quality Indeks Using Long Short Term Memory," *J. Appl. Informatics Comput.*, vol. 8, no. 1, pp. 22–29, 2024, doi: 10.30871/jaic.v8i1.7402.
- [29] X. Wang, J. Wang, Y. Cao, Z. Ye, and W. Zhang, "Principle Analysis of Voiceprint Identification and Authentication System Based on LSTM," *Acad. J. Comput. Inf. Sci.*, vol. 5, no. 7, pp. 85–89, 2022, doi: 10.25236/ajcis.2022.050714.
- [30] J. Wang, S. Hong, Y. Dong, Z. Li, and J. Hu, "Predicting Stock Market Trends Using LSTM Networks: Overcoming RNN Limitations for Improved Financial Forecasting," *J. Comput. Sci. Softw. Appl.*, vol. 4, no. 3, pp. 1–7, 2024, [Online]. Available: <https://mfacademia.org/index.php/jcssa/article/view/100>
- [31] M. A. Moradi, S. A. Sadrossadat, and V. Derhami, "Long Short-Term Memory Neural Networks for Modeling Nonlinear Electronic Components," *IEEE Trans. Components, Packag. Manuf. Technol.*, vol. 11, no. 5, pp. 840–847, 2021, doi: 10.1109/TCPMT.2021.3071351.
- [32] P. Lazcano-Muñoz, "An approach to optimization of Gated Recurrent Unit with Greedy Algorithm," *J. Comput. Forensic Sci.*, vol. 3, no. 1, pp. 22–32, 2024, doi: 10.5937/jcfs3-48703.
- [33] B. Subramanian, B. Olimov, S. M. Naik, S. Kim, K. H. Park, and J. Kim, "An integrated mediapipe-optimized GRU model for Indian sign language recognition," *Sci. Rep.*, vol. 12, no. 1, pp. 1–16, 2022, doi: 10.1038/s41598-022-15998-7.
- [34] C. Ding *et al.*, "Accurate Air-Quality Prediction Using Genetic-Optimized Gated-Recurrent-Unit Architecture," MDPI, pp. 1–21, 2022.
- [35] Z. Liu, W. Li, J. Feng, and J. Zhang, "Research on Satellite Network Traffic Prediction Based on Improved GRU Neural Network," *Sensors*, vol. 22, no. 22, pp. 815–827, 2022, doi: 10.3390/s22228678.
- [36] W. Li, H. Wu, N. Zhu, Y. Jiang, J. Tan, and Y. Guo, "Prediction of dissolved oxygen in a fishery pond based on gated recurrent unit (GRU)," *Inf. Process. Agric.*, vol. 8, no. 1, pp. 185–193, 2021, doi: 10.1016/j.inpa.2020.02.002.
- [37] R. Cahuantzi, X. Chen, and S. Güttel, "A Comparison of LSTM and GRU Networks for Learning Symbolic Sequences," *Lect. Notes Networks Syst.*, vol. 739 LNNS, pp. 771–785, 2023, doi: 10.1007/978-3-031-37963-5_53.